Overview of a CO_2 sequestration field test in the West Pearl Queen reservoir, New Mexico

Rajesh J. Pawar, Norm R. Warpinski, John C. Lorenz, Robert D. Benson, Reid B. Grigg, Bruce A. Stubbs, Philip H. Stauffer, James L. Krumhansl, Scott P. Cooper, and Robert K. Svec

ABSTRACT

Carbon dioxide (CO_2) sequestration in geological formations is the most direct carbon management strategy for reducing anthropogenic CO_2 emissions into the atmosphere and will likely be needed for continuation of the global fossil-fuel–based economy. Storage of CO_2 into depleted oil reservoirs may prove to be both cost effective and environmentally safe. However, injection of CO_2 into oil reservoirs is a complex issue, spanning a wide range of scientific, technological, economic, safety, and regulatory issues. Detailed studies about the long-term impact of CO_2 on the host reservoir are necessary before this technology can be deployed. This article provides an overview of a U.S. Department of Energy–sponsored project that examines CO_2 sequestration in a depleted oil reservoir. The main objectives of the project are (1) to characterize the oil reservoir and its sequestration capacity; (2) to better understand CO_2 sequestration-related processes; and (3) to predict and monitor the migration and ultimate fate of CO_2 after injection into a depleted sandstone oil reservoir. The project is focused around a field test that involved the injection of approximately 2090 tons (2.09 million kg) of CO_2 into a depleted sandstone reservoir at the West Pearl Queen field in southeastern New Mexico. Geophysical monitoring surveys, laboratory experiments, and numerical simulations were performed in support of the field experiment. Results show that the response of the West Pearl Queen reservoir during the field experiment was significantly different than predicted response based on the preinjection characterization data. Furthermore, results from a 19-month bench-scale experiments of CO_2 interaction with the Queen sand were not able to be fully

DOI:10.1306/eg.10290505013

AUTHORS

Rajesh J. Pawar ~ *Earth and Environmental Sciences Division, Los Alamos National Laboratory, MS T003, Los Alamos, New Mexico 87545; rajesh@lanl.gov*

Rajesh Pawar is a technical staff member at the Los Alamos National Laboratory. He received his Ph.D. from the University of Utah in chemical and fuels engineering. His primary research focus is fluid flow in porous media. He has served as the associate editor of *Reviews in Geophysics*.

Norm R. Warpinski ~ *Sandia National Laboratories, Albuquerque, New Mexico; present address: Pinnacle Technologies, Park North Technology Center, 219 Airtex Boulevard, Houston, Texas 77090; nrwarpi@sandia.gov*

Norm Warpinski is currently the chief technology officer for Pinnacle Technologies in Houston, Texas. He is in charge of developing new tools and analyses for hydraulic fracture mapping, reservoir monitoring, hydraulic fracture design and analysis, and integrated solutions for reservoir development. He previously worked at Sandia National Laboratories from 1977 to 2005 on various projects in oil and gas, geothermal, carbon sequestration, waste repositories, and other geomechanics issues. Norm has extensive experience in various types of hydraulic fracture mapping and modeling and has been involved in large-scale field experiments from both the hardware and software sides. He has also worked on formation evaluation, geomechanics, natural fractures, in situ stresses, rock behavior, and rock testing.

John C. Lorenz ~ *MS 0750, Sandia National Laboratories, Albuquerque, New Mexico 87185; jcloren@sandia.gov*

John Lorenz worked for the Peace Corps and the U.S. Geological Survey before joining Sandia National Laboratories in 1981, where he is presently a Distinguished Member of the Technical Staff. He received his Ph.D. from Princeton University, has been elected editor for AAPG, and has published widely on the sedimentology and natural fractures in hydrocarbon reservoirs.

Robert D. Benson ~ *Department of Geophysics, Colorado School of Mines, Golden, Colorado 80401-1887; rbenson@mines.edu*

Robert (Bob) D. Benson is a research associate professor in the Department of Geophysics at the Colorado School of Mines and is codirector of the Reservoir Characterization Project. Benson has more than 25 years of experience in seismic acquisition, processing, and interpretation. He holds B.S. and M.S. degrees and a Ph.D. in geophysics from the Colorado School of Mines. He is a past president of the Denver Geophysical Society.

Reid B. Grigg ~ *New Mexico Institute of Mining and Technology, 801 Leroy Place, Socorro, New Mexico 87801; reid@prrc.nmt.edu*

Reid Grigg is a senior engineer and section head at the New Mexico Petroleum Recovery Research Center and an adjunct professor at the New Mexico Institute of Mining and Technology. His research interests include high-pressure gas-flooding processes, phase behavior, and studies of the fluid properties of high-pressure injection gas and reservoir fluids related to improved oil recovery and carbon storage. He has authored more than 70 publications.

Bruce A. Stubbs ~ *Strata Production Company, Roswell, New Mexico; pecos@lookingglass.net*

Stubbs is a consultant petroleum engineer, with 33 years of industry experience, for Pecos Petroleum Engineering, Inc., in Roswell, New Mexico. He has been a consultant since 1992 after spending 5 years with Hondo Oil and Gas Company. He holds a bachelor's degree in mechanical engineering from the New Mexico State University. He is the project engineer for Strata Production Company on the U.S. Department of Energy Class III Project at Nash Draw.

Philip H. Stauffer ~ *MS T003, Los Alamos National Laboratory, Los Alamos, New Mexico 87545; stauffer@lanl.gov*

Phillip Stauffer is a technical staff member at the Los Alamos National Laboratory. His research involves code development, simulation, and assessment of subsurface multiphase transport in a variety of geological environments. His background in heat and mass transport includes work on the Yucca Mountain Project, the Ocean Drilling Program, and most recently, the Zero Emissions Research and Technology Program.

James L. Krumhansl ~ *MS 0754, Sandia National Laboratories, Albuquerque, New Mexico 87185; jlkrumh@sandia.gov*

Jim is a principal member of the Sandia National Laboratories scientific staff, where he has worked since he received his Ph.D. in geology from Stanford University in 1976. His expertise is environmental and aqueous geochemistry, where he has applied numerous issues, including the Waste Isolation Pilot Project (WIPP) and the Yucca Mountain Project (YMP).

Scott L. Cooper ~ *MS 0750, Sandia National Laboratories, Albuquerque, New Mexico 87185; spcoope@sandia.gov*

Scott Cooper is a senior member of the technical staff at Sandia National Laboratories. He received his B.S. degree from the South Dakota School of Mines and Technology (1997) and his M.S. degree in geology from the New Mexico Institute of Mining and Technology (2000). His current research focuses on natural fracture systems and reservoir characterization.

Robert K. Svec ~ *New Mexico Institute of Mining and Technology, 801 Leroy Place, Socorro, New Mexico 87801*

Bob Svec received his bachelor's degree in physics and his master's degree in geophysics from the New Mexico Institute of Mining and Technology. His current research interests lie in high-pressure experiments including CO_2 core flooding and reservoir characterization.

ACKNOWLEDGEMENTS

Funding for this work was provided by the U.S. Department of Energy. The authors also thank KinderMorgan CO_2 for donating the CO_2 used during field-injection experiments.

reproduced using the latest numerical modeling algorithms, suggesting that the current models are not capturing important geochemical interactions.

INTRODUCTION

Among the most direct methods to sequester CO_2 is its injection into geological formations. Deep saline aquifers, uneconomic coal seams, and depleted gas reservoirs are potential options; however, depleted oil reservoirs are available for immediate deployment of this technology. Depleted oil reservoirs have distinct advantages over other geological storage options.

- Knowledge base: A large number of oil reservoirs have already been extensively characterized. Most of the characterization information for oil fields in the United States and elsewhere is publicly available. Additionally, the use of CO_2 in enhanced oil recovery (EOR) operations for more than three decades has resulted in information on interactions between CO_2 and reservoir rock and fluids that could be useful in estimating capacity and predicting the long-term fate of CO_2.
- Infrastructure: A major advantage of oil and gas reservoirs is that numerous wells have been drilled in these fields. A large percentage of these wells have the potential to be converted to injection and/or monitoring wells. In addition, CO_2-EOR operations have also resulted in pipeline infrastructure for transporting CO_2, most extensively in the Permian Basin in west Texas.
- Economics: Depleted oil reservoirs have the potential for incremental oil recovery that can considerably improve the overall economics for CO_2 sequestration projects.

There are also some disadvantages to depleted oil reservoirs. Based on the initial estimates, these reservoirs have lesser capacity compared to saline aquifers. In addition to the existing wells, these reservoirs have a large number of abandoned wells. In some cases, the locations of these wells are unknown. Depending on the quality of abandonment, these wells may become potential future pathways for escape of CO_2 from the reservoir.

Before geological sequestration of CO_2 can be used on large scales, confidence in this technology needs to be ensured by addressing safety issues, developing a proper regulatory regime, and better evaluating the overall economics. Ensuring confidence requires undertaking projects with specific sequestration-related objectives. In the case of oil reservoirs, this would require projects that are not typical (e.g., oil production-driven) EOR projects. Current industrial EOR reservoir strategies, which include uniform flood sweep, optimized placement of wells, inhibition of viscous fingering, and minimizing CO_2 injection (Mungan, 1992), are based on economic goals that are not well aligned with sequestration goals.

Sequestration goals are targeted to enhance sequestration volume and duration of CO_2 in geological formations. In the past, there have been few economic incentives and minimal research-and-development support to understand the physical and chemical interactions and ultimate fate of injected CO_2 in oil-producing reservoirs during EOR sweeps.

Our project aims to provide important elements of the science and technology base that will be necessary to properly evaluate the safety and efficacy of long-term CO_2 sequestration in depleted oil reservoirs. The results and data generated in this project will be valuable in assessing other geological reservoirs. The ultimate goal of the project is to predict the migration and long-term fate of CO_2 in sandstone oil reservoirs. Although the ultimate goal of such studies is to improve our understanding of the main sequestration mechanisms and resultant reservoir processes, a complete assessment of geological sequestration will require several similar test programs to assess different geological settings. The project is a multiorganizational effort that includes United States national laboratories, academia, and industry. The primary partners include the Los Alamos National Laboratory, Sandia National Laboratories, Strata Production Company, the New Mexico Institute of Mining and Technology, and the Colorado School of Mines. The project combines a small-scale field-injection experiment with geophysical monitoring, numerical simulation, and laboratory experiments, with the following objectives:

- characterization of the oil reservoir and its capacity to sequester CO_2
- characterization of the interactions of CO_2 with reservoir fluids and rocks
- assessment of the ability of geophysical techniques to monitor

The project is divided into three phases:

- Phase I consisted of preinjection activities, including characterization of the reservoir, calculation of expected CO_2 injection and migration behavior, acquisition of baseline geophysical surveys, preparation of the injection well, and acquisition of legal permits for injection.
- Phase II consisted of activities pertaining to the injection and soaking of CO_2 in the reservoir; these included the design of the field-injection test, preparation of surface injection facilities, injection of CO_2, measurement of reservoir pressure changes, acquisition of geophysical surveys, postsoaking CO_2 production, and refinement of computer-simulation models.
- Phase III consisted of activities related to predicting CO_2 migration and its interaction with the reservoir rocks and fluids, including acquisition of postsoak geophysical surveys, venting of CO_2 from the reservoir, monitoring gas and liquid production, collection and analysis of gas and liquid samples, iteration of computer-simulation models, and integration of the results, analyses, and data from the project.

We are currently continuing work in phase III, monitoring CO_2 migration in the reservoir, and are integrating the data acquired to understand CO_2 migration. This study provides details of the preinjection characterization activities and the field experiments. Details of the integration of data and modeling results and CO_2 migration will be published at a later date.

FIELD SITE

We chose the West Pearl Queen depleted oil reservoir for the field test. It is located in southeastern New Mexico (Figure 1) and is operated by the Strata Production Company (SPC) of Roswell, New Mexico. This field had some distinct advantages, including

- no economic and technical restrictions of an EOR operation
- opportunity and freedom to observe the response of the reservoir without the concerns of early breakthrough or degradation of production reservoir features
- availability of offset wells for monitoring instead of production of oil
- ability of varying soak times beyond industry EOR standards

The field has produced about 250,000 bbl (39,746 m^3) of oil since 1984. Production from the field has slowed in recent years. No secondary or tertiary recovery operations have been applied in the field, which made this field an attractive field site because the interpretation of field experiment results would not have the complications related to the prior enhanced recovery operations.

Figure 2 shows a site map with the locations of wells in the field. The field is primarily located in Sec. 27, 28, and 33, T19S R34W. Strata Production Company has drilled five wells in the field. Of the

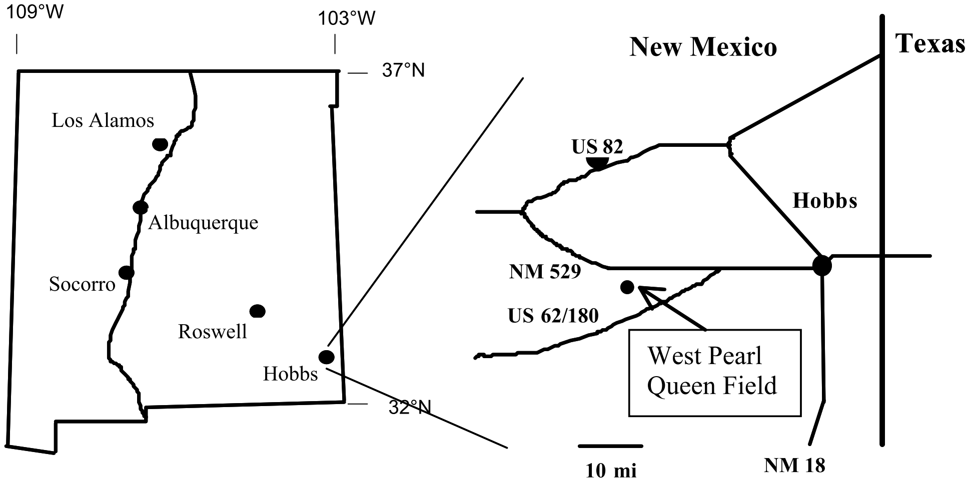

Figure 1. Location of the West Pearl Queen field, southeastern New Mexico. The reservoir strata are 4500 ft (1371 m) below the surface geology, which consists of poorly and unconsolidated Tertiary and Quaternary sediments.

five wells, currently, only Stivason Federal 5 is actively produced. Wells Stivason Federal 1 and Stivason Federal 3 have been recently converted into produced-water disposal wells. Well Stivason Federal 2 has been shut in. Well Stivason Federal 4, which has been shut in since 1998, was chosen as the CO_2-injection well for the field experiment. Production from Stivason Federal 5 was stopped during the field experiment, and the well was available for monitoring and for cross-well surveys. Figure 2 also shows other wells in the area. Of these, only well Sun Pearl 2 is completed in the Queen Formation.

PREINJECTION CHARACTERIZATION

Preinjection characterization of the field included several activities. The goal was to characterize the reservoir geology, reservoir-flow dynamics, and the potential response of reservoir rock to CO_2 injection.

Geology

Several techniques and data sources were used to characterize reservoir geology. Prior to this project, data available to characterize the reservoir geology were

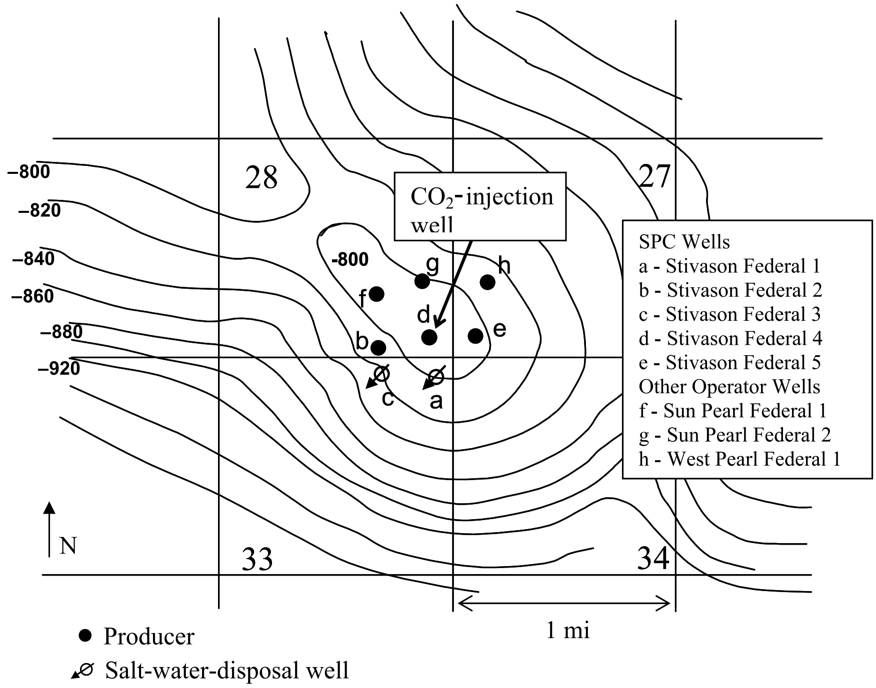

Figure 2. Structure-contour (subsea-depth) map of the West Pearl Queen field based on well picks at the top of the Shattuck Member of the Queen Formation. It is significantly different from the structure map based on seismic data presented later (Figure 8). This figure shows the locations of the wells pertinent to this study, including the production and water-injection wells, the central CO_2-injection well, and the monitor well.

limited and primarily consisted of logs, including gamma ray, neutron porosity, density porosity, and dual laterologs (resistivity). In addition, results of core analyses, which consisted of porosity and permeability measurements for well Stivason Federal 1, were also available. No seismic surveys were acquired for the field prior to this project; hence, several activities were performed to further characterize the reservoir structure and geology. We were successful in obtaining actual core from the reservoir. A detailed analysis using the core, historic logs, and outcrop was performed. In addition, several geophysical surveys were acquired, including dipole sonic logs for wells Stivason Federal 4 and Stivason Federal 5; a cross-well survey between wells Stivason Federal 4 and Stivason Federal 5; and a high-resolution, three-dimensional, nine-component surface seismic survey. The surface seismic survey employed about 1000 source and receiver locations and covered an area of 1 mi^2 (2.6 km^2) around well Stivason Federal 4. The survey was repeated during the field experiment to monitor CO_2 migration. Both the repeat survey and the baseline survey were used to interpret the structure. The surveys had uniform azimuth and offset distribution and provided high-resolution coverage. Because time-lapse effects are subtle, the surveys were designed to maximize the signal-to-noise ratio of the data and its repeatability. In processing, surface-consistent linear processes were used, thereby preserving the integrity of the signal between the baseline and monitor surveys.

The West Pearl Queen field reservoir is in the Permian–age Shattuck Member of the Queen Formation. It is a sandy, shaly, and evaporitic unit deposited in ephemeral flood-plain fluvial environments at the margin of the Permian Basin (Holley and Mazzullo, 1988; Malicse and Mazzullo, 1990; Mazzullo et al., 1991). The average depth of the reservoir is about 4500 ft (1371.6 m). The average gross thickness of the reservoir is about 40 ft (12.2 m). Analysis of core shows three basic lithologies. About 80% of the available core consists of poorly cemented, oil-stained sandstone with 15–20% porosity and highly variable permeability up to 200 md (2×10^{-13} m^2). It is a cross-bedded to massive, arkosic, and fine- to very fine-grained sandstone. Oil staining and laboratory measurements indicate high porosity, and the three zones composed of this facies probably constitute the primary reservoirs. Several nonreservoir lithologies separate the zones of good reservoir properties. One common facies consists of thinly bedded sandstone to siltstone. The other common facies consists of laminated to massive, very fine-grained, light-gray sandstones.

Geophysical logs show that the reservoir is divided into three main high-porosity zones (Figure 3). In certain locations, one of the zones is further divided into two zones. Mineralogical analysis of the core shows that the good reservoir is a fine-grained, friable sandstone containing a preponderance of quartz, with lesser amounts of detrital K-feldspar and Na-rich plagioclase grains. The formation is cemented by prominent overgrowths of very pure euhedral, diagenetic K-feldspar and Mg-rich calcite (Figure 4). Any clays that may have been initially present were apparently obliterated by the diagenetic processes that gave rise to the K-feldspar and carbonate mineral overgrowths.

A P-wave tomogram from the cross-well survey is shown in Figure 5. In addition to the tomogram, derived velocity logs (red) and measured velocities using a dipole sonic log (black) are also shown. The West Pearl Queen Formation is the low-velocity zone between 4500- and 4600-ft (1371.6- and 1402.1-m) depth. The individual productive zones in the reservoir cannot be distinguished with the cross-well survey.

As mentioned earlier, both sets of three-dimensional surface seismic surveys were used to interpret the geological structure. Cross-equalization of the baseline and monitor seismic surveys was a critical part of the analysis. Figure 6 shows the reservoir interval on the baseline survey and both the matched and unmatched monitor surveys. Subtle differences are observed above the reservoir on the unmatched survey, and these differences were removed on the cross-equalized survey. The Queen Formation was interpreted as a trough between 740 and 758 ms, representing the Seven Rivers–Queen lithofacies change from carbonate to siliciclastic rocks. The time-structure map and edge-detection maps created from the P-wave seismic data on the reservoir interval characterize a sand-filled incised paleochannel and some paleohighs associated with the dome structure, as originally interpreted from the well data. The depth-structure map of the West Pearl Queen reservoir differs significantly from the time-structure map, showing an anticlinal structure to the east of the CO_2-injection well (Figure 7). Figure 8 shows the RMS (root-mean-squared) amplitude map. Both the cross-well survey and RMS amplitude map show that the reservoir is heterogeneous between wells Stivason Federal 4 and Stivason Federal 5.

Outcrops of the Shattuck Member sandstones approximately 50 mi (80 km) to the west but in the same position several miles landward of the Goat Seep reef contain two prominent and consistent fracture sets, but neither core nor well tests indicate the presence or

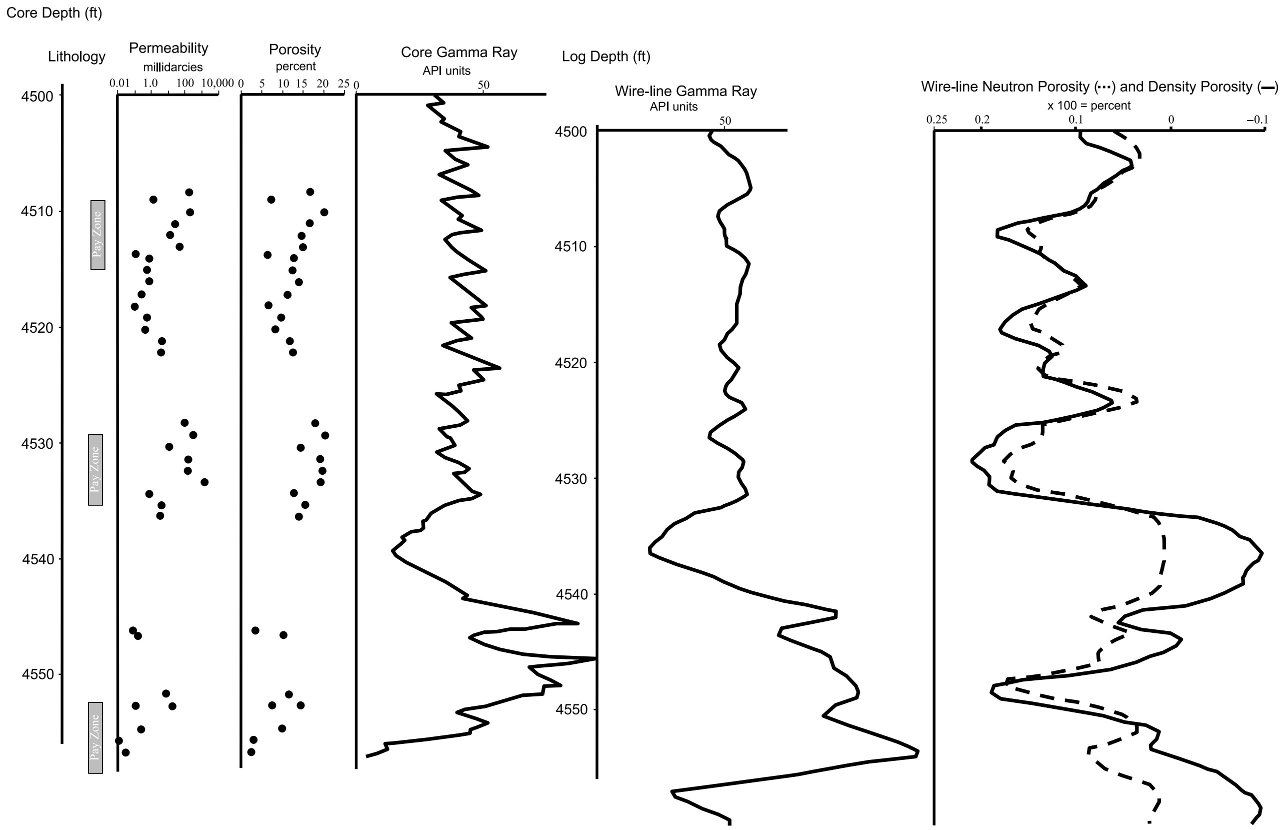

Figure 3. Comparison of core data and wire-line-log data for well Stivason Federal 1. Poor gamma-ray differentiation of units reflects the high potassium-feldspar content of the sandstones. Large sections of the core were missing by the time of this study, but records of the porosity and permeability data were found for some of the missing intervals. The three high-porosity zones depicted that both the neutron and density porosity logs (right scale) have been used in the modeling effort. A 10–12-ft (3–3.6-m) depth shift exists between the core and wire-line data.

influence of natural fractures in the subsurface reservoirs of the West Pearl Queen field. Similarly, the seismic data do not show the presence of any major faults in the reservoir, suggesting that there are no structural complications that would compartmentalize or divert injected CO_2.

Laboratory Experiments

To characterize the reservoir rock and fluids and to understand the impact of CO_2 on reservoir rock properties, two separate types of laboratory experiments were performed.

1. Static experiments: These experiments were performed to characterize the geochemical interactions between reservoir rock, formation brine, and CO_2. Injection of CO_2 leads to lowering the pH of formation brine and may initiate geochemical reactions. The geochemical reactions could either lower

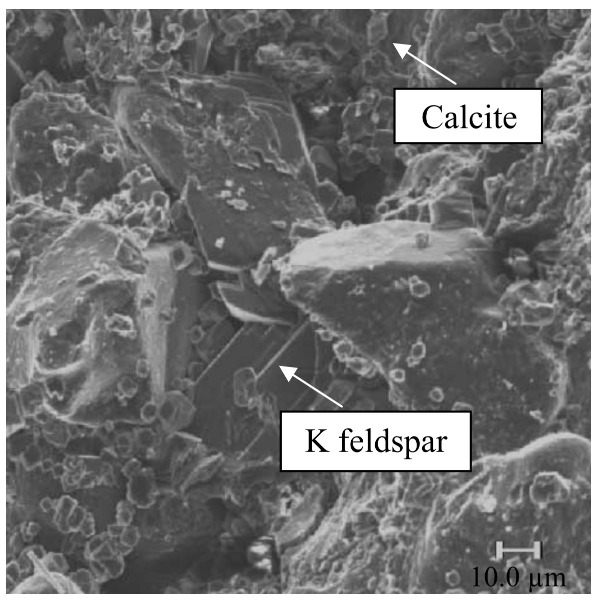

Figure 4. Scanning electron microscopy photograph of a West Pearl Queen reservoir rock sample prior to being exposed to CO_2. Calcite cements and potassium feldspars are fresh and unaltered.

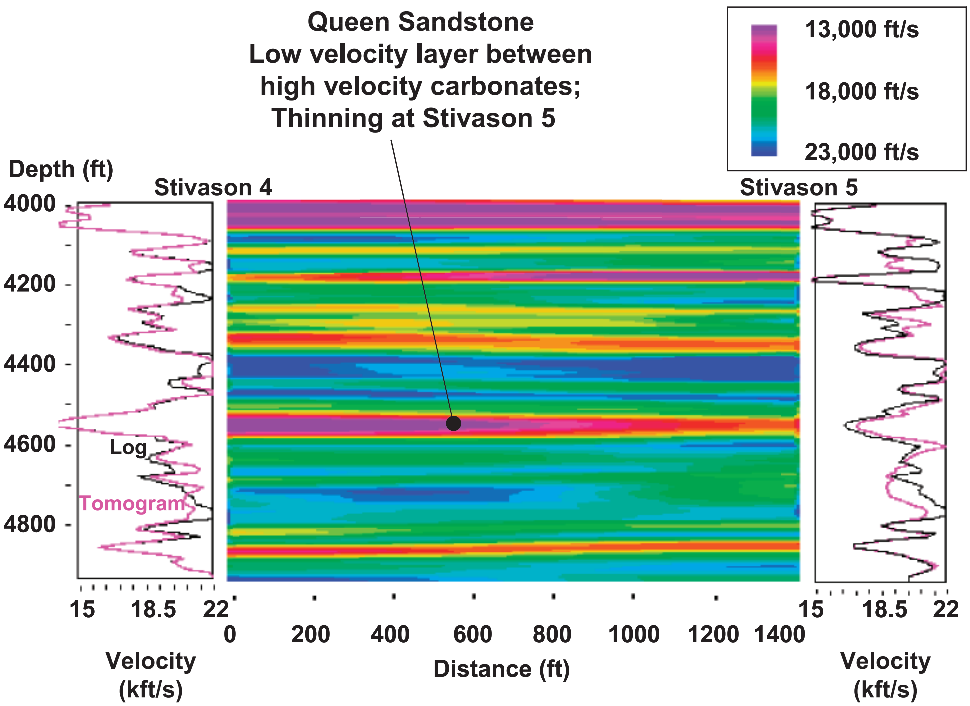

Figure 5. Tomogram of P-wave (center) and derived and measured log velocities (sides) for preinjection cross-well survey between wells Stivason Federal 4 and Stivason Federal 5.

formation porosity and permeability by precipitating new minerals or increase porosity and permeability by dissolving mineral phases. In the long term, geochemical interactions can lead to chemical fixation of CO_2 in the form of a stable mineral phase. It is crucial to determine what types of geochemical reactions are occurring as well as what the kinetics of the reactions are. These questions were addressed by a combination of laboratory experiments and numerical modeling. The laboratory experiments were relatively short term (months) and were most applicable to predicting what changes might have happened in the field experiment time frame. During the experiments, a few tenths of a gram of sandstone was placed in a stainless-steel autoclave with 3 mL of formation brine, and subjected to 700 psig (4.8 MPa) of CO_2 pressure at 40°C. After 19 months, both the fluid and rock samples were examined. The present-day indigenous brine is essentially a sodium (52 ppt)-chloride (109 ppt) brine, with lesser amounts of

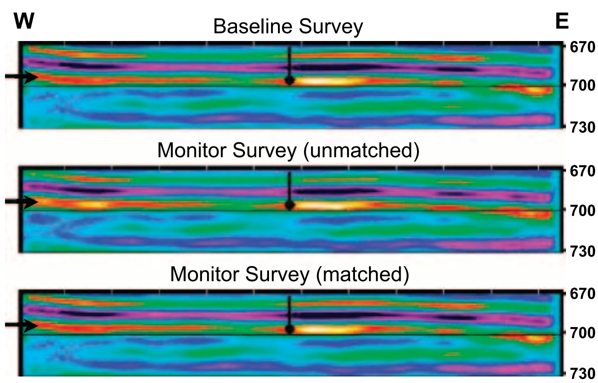

Figure 6. Cross section showing the West Pearl Queen reservoir based on the baseline and matched and unmatched monitor three-dimensional seismic survey.

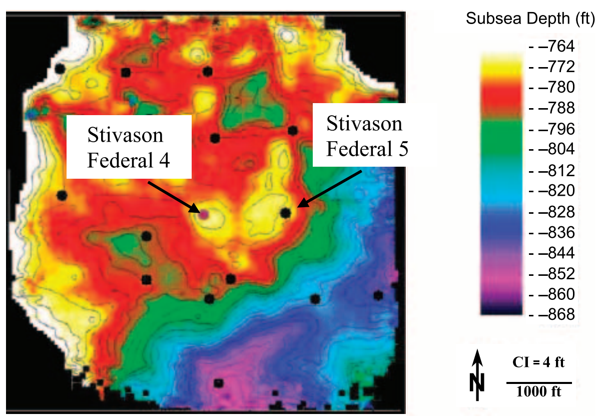

Figure 7. Depth-structure map of West Pearl Queen reservoir based on seismic two-way traveltimes converted to depth using the log-derived velocity model.

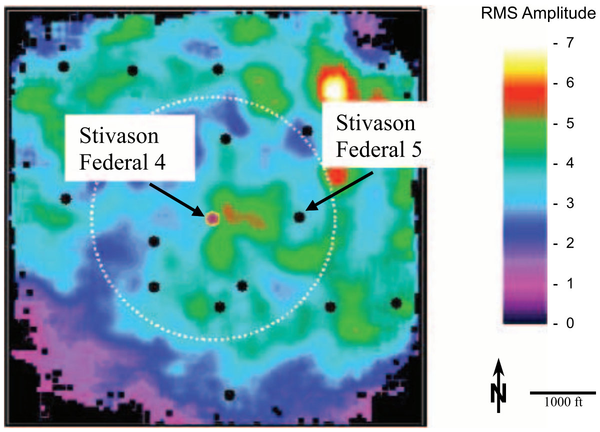

Figure 8. Root-mean-squared (RMS) amplitude map of the West Pearl Queen reservoir. Variability in the amplitude represents heterogeneity in the reservoir.

dissolved potassium (1.6 ppt), magnesium (3.1 ppt), calcium (also 3.1 ppt), sulfate (1.8 ppt), and bicarbonate (0.12 ppt). Post-test fluid analysis showed that the dissolved Ca levels had increased by 23%, and that of Mg had increased by 35%. Dissolved silicon (not silica) dropped from 12.3 to 3.6 ppm, whereas aluminum concentration increased from 0.05 to 0.33 ppm. Considering the amounts of alkali metals (Ca, Mg) initially present in the brine relative to the amounts of silicon and aluminum, it would be reasonable to surmise that most of the short-term changes in the formation chemistry would involve the removal of the carbonate minerals. In fact, all of the calcite and virtually all of the more Mg-rich dolomitelike phase were removed during the course of the experiment. Diligent examination of the samples, however, also revealed some etching of the plagioclase feldspars, as well the beginning of clay precipitation (Figure 9). The K-feldspars were not affected by the treatment. The laboratory experiments suggested that dawsonite might not form during the field test. Early formation of clays was relatively slow compared to the duration of the field test. These results indicate that the probable geochemical alterations during the field test will not affect reservoir transport properties.

2. Flowthrough experiments: These experiments were performed with samples from the reservoir core representing several possible producing zones (Table 1) to test for porosity, permeability to brine, and relative permeability to brine and CO_2 (the relative permeability measured in these experiments did not include three-phase relative permeability in the presence of oil). As can be seen from Table 1, the permeability varied from high to low within a short distance. Figures 10 and 11 represent the relative permeability curves for core plugs at 4510.5 ft (1374.8 m) depth. Each of these measurements was performed at 114°F (45.5°C) and at two pore pressures, 500 and 2000 psig (3.4 and 13.8 MPa). The differences in the two figures are primarily caused by differences in pressure. The difference in pressure results in large differences in the density of CO_2, solubility of water in CO_2 and CO_2 in brine, and surface tension between the phases. Figure 12 shows changes in porosity and permeability with time because of the effects of two-phase flow of brine and CO_2. The figure shows porosity and permeability versus pore volumes of fluid injected. It is interesting to note that, with time, porosity increased, whereas permeability decreased. A possible explanation for this could be that geochemical reactions with CO_2 have freed cemented fines that migrated and got stuck in pore throats, thus reducing the permeability. In each of the tests, the irreducible brine saturation was between 60 and 70% when using CO_2 to reduce brine saturation in a core 100% saturated with brine. Figure 13 shows the amount of brine

Figure 9. Scanning electron microscopy photographs of West Pearl Queen reservoir sandstone after 19 months exposure to high-pressure CO_2 gas. The potassium feldspars (left) have not been affected, whereas the sodium and calcium feldspars have started to etch (middle), and authigenic clays derived from dissolution of these components have started to form (right).

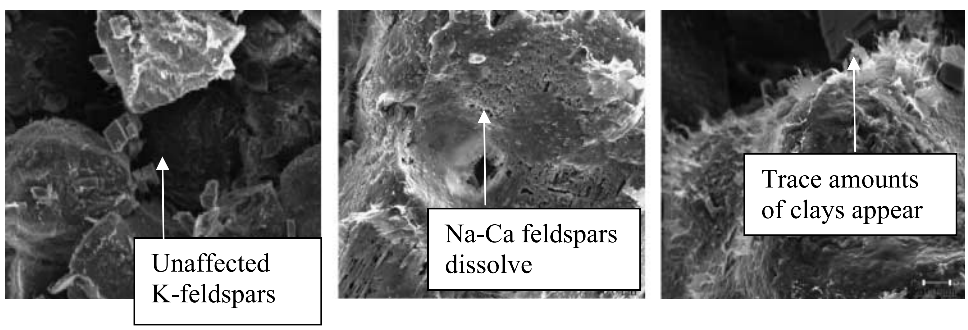

Table 1. Rock Properties from West Pearl Queen Reservoir Core Samples

Core Depth (ft)	Permeability to Brine (md)	Porosity (%)
4508.9	<<1	
4510.5	160	21.7
4511.2	15.8	18.1
4513.0	2.62	14.0
4532.5	117	20.5
4532.7	<1	

produced because of CO_2 injection during a laboratory core-flooding experiment. After 4000 cm^3 (244 $in.^3$) of CO_2 (at reservoir conditions) had been injected, 0.62 PV (pore volume) of brine was left behind in sample 4532.5.

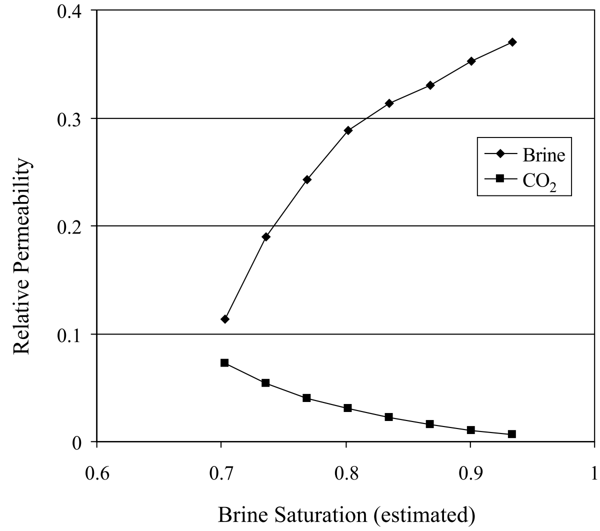

Figure 11. Relative permeability curve for core plug 4510.5 at 2000 psig (13.8 MPa). At higher pressures, the relative permeability to CO_2 decreases significantly as brine saturation increases.

Numerical Simulations

Two types of numerical simulations were performed, including flow simulations and geochemical reaction simulations. The overall goal of numerical simulations is to predict the long-term migration and the fate of CO_2 in the reservoir. The goal of the preinjection numerical simulations was to characterize the reservoir-flow dynamics, as well as the geochemical interactions. Results of these simulations were used to understand the laboratory experiment results and to predict field experiment behavior.

1. Reservoir-flow simulations. These simulations were performed to characterize the overall flow behavior of the reservoir. Preinjection simulations were also used to determine whether the proposed amount of CO_2 could be injected in the target interval given the operational and regulatory constraints. The regulation required the injection to be performed at a rate

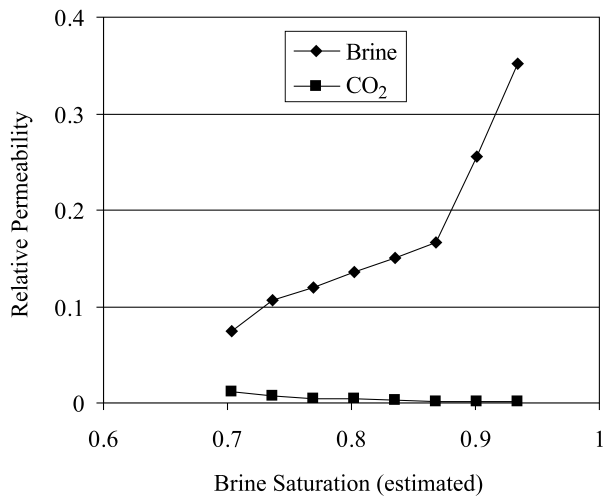

Figure 10. Relative permeability curve for core plug 4510.5 at 500 psig (3.45 MPa). The relative permeability to CO_2 decreases slightly as brine saturation increases.

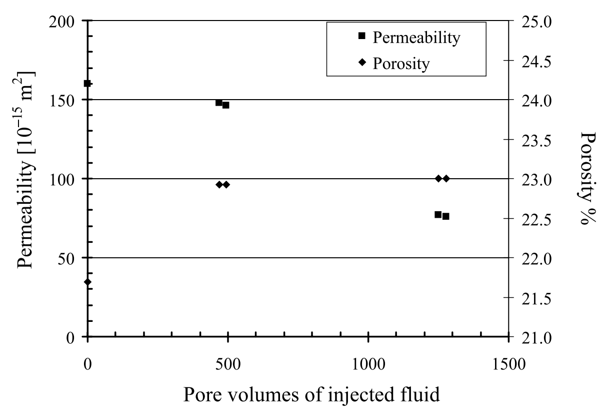

Figure 12. Change in core porosity and permeability during CO_2 injection in laboratory experiments. Permeability decreased by more than 50%, possibly because of growth and migration of clays, whereas porosity, initially increasing by several percent because of dissolution, stabilized.

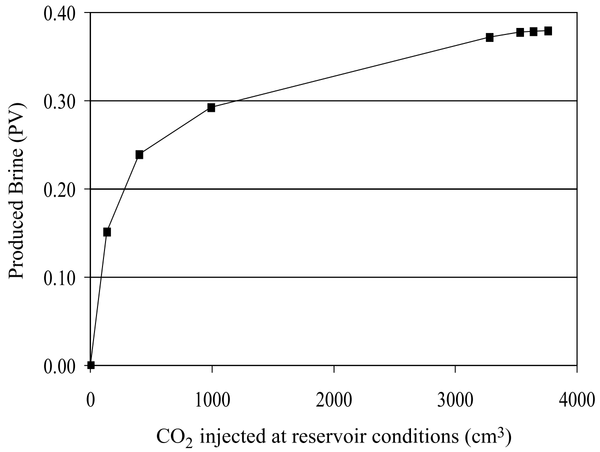

Figure 13. Amount of brine produced during CO_2 injection in laboratory experiment for core 4532.5 (20 cm^3 [1.22 $in.^3$] ~1 PV). The core was initially saturated with brine. Even after injection of almost 200 PV of CO_2, a significant amount of brine (~0.63 PV) is left behind in the core.

such that the bottom-hole pressure does not exceed the rock-fracturing pressure. Based on the prevailing lithostatic pressure gradient, 0.64 psi/ft (14.5 kPa/m), and depth of the injection interval, this pressure was determined to be about 2900 psi (19.9 MPa) at the bottom hole. In addition, the simulations were also used to determine the possible migration of CO_2 after injection. A numerical model for the reservoir was developed based on the geological characterization. At the time the preinjection simulations were performed, geophysical surveys were not acquired; hence, only the data based on log and core analysis were used to develop the flow model. The numerical simulations were run using Eclipse, Schlumberger's oil reservoir simulator. The flow model was validated through matching the historic production data and then used to perform CO_2-injection simulations. These simulations were performed using the compositional module. Compositional simulations consider thermodynamic interactions between the hydrocarbon components present in the reservoir. Several simulation runs were performed to characterize the reservoir response to varying injection conditions. The simulations were run to model the injection as well as subsequent soak and venting operations of the field experiments. The simulation results indicated that CO_2 could be injected in the reservoir at a rate of 100 t/day (100,000 kg/day) without exceeding the bottom-hole pressure constraint. It was also estimated that the CO_2 plume would reach the monitoring well (Stivason Federal 5) during the 6-month soak period. Simulation of the venting operation suggested that about half of the injected CO_2 could be produced from the reservoir in the first 6 months of venting.

2. Geochemical simulations. Two types of numerical models were used to characterize the geochemical interactions. The first model, REACT, was used to predict the most stable configuration of the system after equilibrium has been achieved along a reaction path with the steady addition of CO_2. The second numerical model, FLOTRAN (flow and transport simulator) (Lichtner, 2001), was used to explore both short- (months) and long (more than 1000-yr)-term geochemical behavior. The model REACT was used to study a system containing minerals and brine with compositions similar to the reservoir rock and brine and in proportions closer to what may be present in the reservoir (Table 2). Model predictions showed that this system could result in precipitation of large amounts of dawsonite [$NaAlCO_3(OH)$] (Figure 14). In addition, kaolinite would be formed from the reaction of albite. The brine-to-mineral ratio was varied to more closely reflect the conditions in the laboratory experiments mentioned earlier. This system predicted reaction products similar to the ones observed in the laboratory experiments, including the early appearance of some clay, the disappearance of calcite, and the partial early attrition of albite (Figure 15). However, the results of the model, having a more formationlike rock-to-brine ratio, suggest that the appearance of clays in the laboratory experiments should not be taken as a potential indicator that they would appear either throughout the long term in a sequestration setting or in the short term in a field test. The most important part of these calculations is the ubiquitous prediction that significant amounts of dawsonite will accompany the breakdown of feldspars.

Table 2. Proportion of Brine and Minerals Used for REACT Simulations

Component	Weight (kg)
Brine	1.0
K-feldspar	1.9
Quartz	10.3
Albite	2.5
Anorthite	12.5
Calcite	0.15
CO_2	0.6

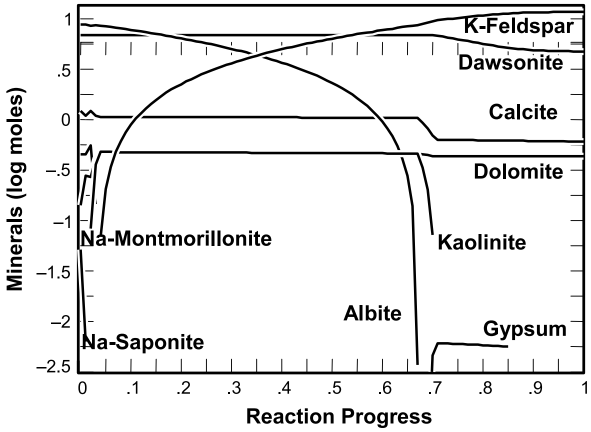

Figure 14. Calculation of minerals that would be formed because of CO_2 reaction with West Pearl Queen reservoir sandstone and brine using a mineral-to-brine ratio similar to that found in the actual reservoir.

Simulations with FLOTRAN were used to match observations of the laboratory experiment after 19 months. To match the experiment results, values of the kinetic constants at 25°C, k_{25} (mol/cm^2 s), and the mineral surface areas (m^2/g) were varied. Values of surface areas and the reaction parameters were obtained from literature (Rimstidt and Barnes, 1980; Knauss and Wolrey, 1986; Fetter, 1999; and Xu et al., 2003). Table 3 lists the allowed mineral phases and the associated variable parameters used to generate the best fit to the experiment. The initial water/rock ratio was set to 3.16. Similar to REACT simulations, this system also resulted in the formation of dawsonite. To match the laboratory observations, the formation of dawsonite and chalcedony had to be suppressed (to allow formation beidelite-Na, which may be the clay mineral observed in the SEM images in Figure 9), and the kinetic rate constant, k_{25}, for K-feldspar had to be reduced from 10^{-16} to 10^{-17} (mol/cm^2 s). Figure 16 shows the pre- and postexperiment major ion brine chemistry for both the laboratory experiment and the simulated experiment. Most of the experimental results are captured in this simulation; however, we were not able to lower the total Al^{3+} in solution to the levels seen in the experiment. In addition, the simulations predict slightly more aqueous SiO_2 than that seen in the experiment. This model was used to predict the long-term geochemical behavior by performing a 1000-yr simulation. For this model, the water/rock ratio was changed to 0.176, closer to that expected in the field. Figure 17 shows the time history of mineral formation and dissolution throughout 1000 yr. The results show that quartz, dolomite, and kaolinite precipitate. Initially, calcite precipitates, but after 50 yr, it dissolves slowly. Potassium-feldspar remains unaltered, whereas beidelite-Na initially precipitates until approximately 50 yr and then rapidly dissolves. Total porosity in the simulation dropped from 0.15 to 0.146, which implies that significant changes in the porous medium will not occur. The fugacity of CO_2 dropped from 48.26 to a value of 0.31 after 1000 yr. This means that the pure-phase CO_2 has been converted into both minerals (calcite, dolomite, and kaolinite) and aqueous carbonate species.

FIELD EXPERIMENT

The central part of the project was the characterization of field response to CO_2 through a field experiment. The field experiment consisted of three steps: injection, soak, and venting. The total duration of the test from the beginning of the injection to the initial venting was about 11 months. Details of each of these steps follow.

Injection

The injection consisted of 2090 t (2.09 million kg) of CO_2 throughout a period of 50 days, between December 20, 2002, and February 11, 2003. As mentioned earlier, CO_2 was injected through well Stivason Federal 4. Based on preinjection characterization, the expected rate of injection was about 100 t/day (100,000 kg/day). This rate was estimated based on the bottom-hole pressure upper-limit constraint of 2900 psi (19.9 MPa).

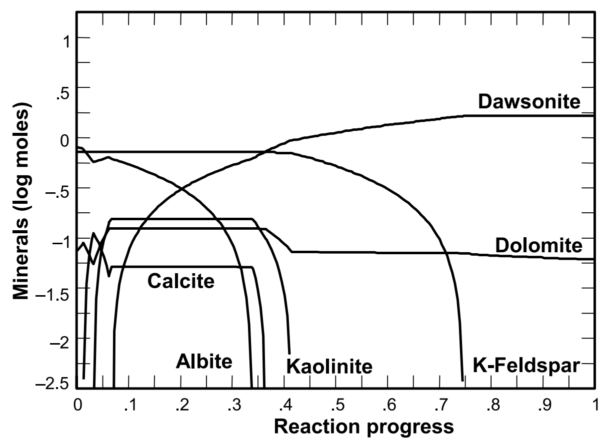

Figure 15. Calculation of minerals that would be formed because of CO_2 reaction with West Pearl Queen reservoir sandstone and brine using a mineral-to-brine ratio similar to that used in the laboratory experiment.

Table 3. Best-Fit Parameters Used for FLOTRAN Simulations of the Bench-Scale Experiment for All Mineral Phases Allowed in the Simulation

	Surface Area (cm^2/g)	Log k_{25} (mol/[cm^2 s])	Initial Volume Fraction Bench Scale	Initial Volume Fraction Field Scale	Final Volume Fraction Field Scale (pH = 6.6)
Albite	6×10^2	10^{-16}	0.07	0.136	0.125
Anorthite	6×10^2	10^{-16}	0	0.007	0.0
Quartz	5×10^2	$10^{-17.9}$	00.129	0.587	0.591
SiO_2 amorphous	1×10^5	$10^{-15.6}$	0	0	0
K-feldspar	3×10^2	10^{-17}	0.042	0.118	0.119
Magnesite	3×10^4	10^{-15}	0	0	0
Kaolinite	3×10^5	10^{-17}	0	0	1.18×10^{-2}
Dolomite-dis	3×10^4	$10^{-18.2}$	0.0001	4.25×10^{-4}	1.85×10^{-3}
Calcite	3×10^3	$10^{-12.8}$	0.00043	1.53×10^{-3}	3.82×10^{-3}
Beidelite-Na	3×10^5	10^{-17}	0	0	0
Gypsum	1×10^5	10^{-13}	0	0	0

During injection, the surface injection pressure quickly reached 1400 psi (9.6 MPa). Based on the surface pressure, the bottom-hole pressure was estimated to be about 2900 psi (19.9 MPa), and the surface injection pressure was not increased above this value. The injection rate was about 200 bbl/day, which translated to 40 t/day (40,000 kg/day). This rate was significantly lower than the preinjection estimates. The surface injection pressure remained constant throughout injection, and the rate of injection could not be increased. Figure 18 shows the pressure, injection rate, and cumulative injected CO_2 during the experiment. We also deployed a passive seismic monitoring technique during injection. A receiver array was deployed in well Stivason Federal 5, and the microseisms generated during injection were recorded. Analysis of the data did not show any significant microseismic events, suggesting that the injection rate was not high enough to cause any significant fracturing. The lower-than-expected injection rate suggests that the reservoir permeability was lower than estimated, and that the reservoir pressure was higher than expected.

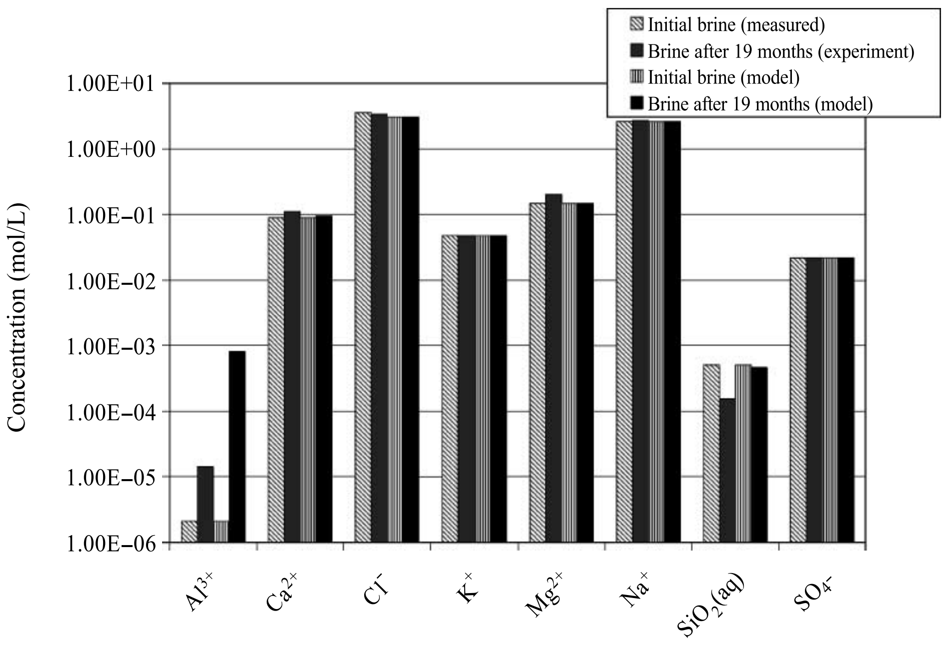

Figure 16. Comparison of FLOTRAN results with geochemical laboratory experiment results after 19 months. Dawsonite and chalcedony formation had to be suppressed to make the model ("model") match the laboratory results ("measured" and "experiment").

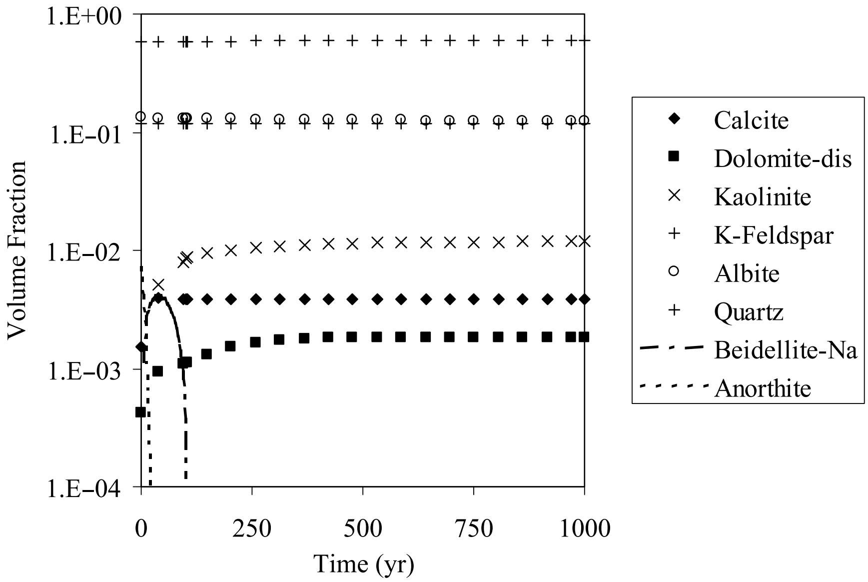

Figure 17. FLOTRAN predictions of geochemical reaction products after 1000 yr. Most changes occur within the first 150–200 yr, when kaolinite and dolomite precipitate while anorthite dissolves. Beidellite-Na initially precipitates but then dissolves.

Soak

At the end of injection, a downhole pressure monitor was deployed in the injection well, and the well was shut in for 6 months. The pressure in the reservoir was monitored intermittently. The measured reservoir pressure is shown in Figure 19. As can be seen from the figure, the pressure near the injection well did indeed reach 2900 psi (19.9 MPa). The pressure reached an asymptotic value after the initial drop-off, indicating that steady state was reached. The equilibrium pressure value was about 1700 psi (11.7 MPa), which was significantly higher than earlier predictions. Carbon dioxide was allowed to soak for 6 months, at the end of which, another three-dimensional, multicomponent seismic survey was acquired. As mentioned earlier, this monitoring survey had the same attributes as the baseline survey.

Venting

After acquisition of the postinjection seismic survey, CO_2 was vented from well Stivason Federal 4. The well was connected to a separator and a fluid collection

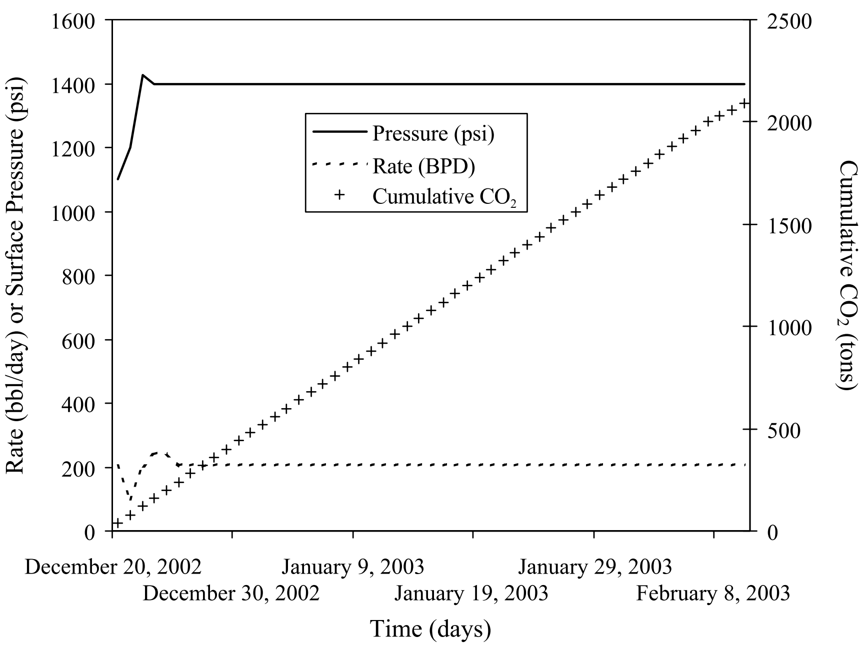

Figure 18. CO_2-injection parameters during field injection experiment. The injection rate stabilized at 40 tons/day (200 bbl/day), well below the expected 100 tons/day, because injection pressures were much higher than expected.

Figure 19. Bottom-hole pressure in well Stivason Federal 4 during the post-injection soak period, showing that the reservoir pressure was nearly stabilized at equilibrium 2 months after shut-in.

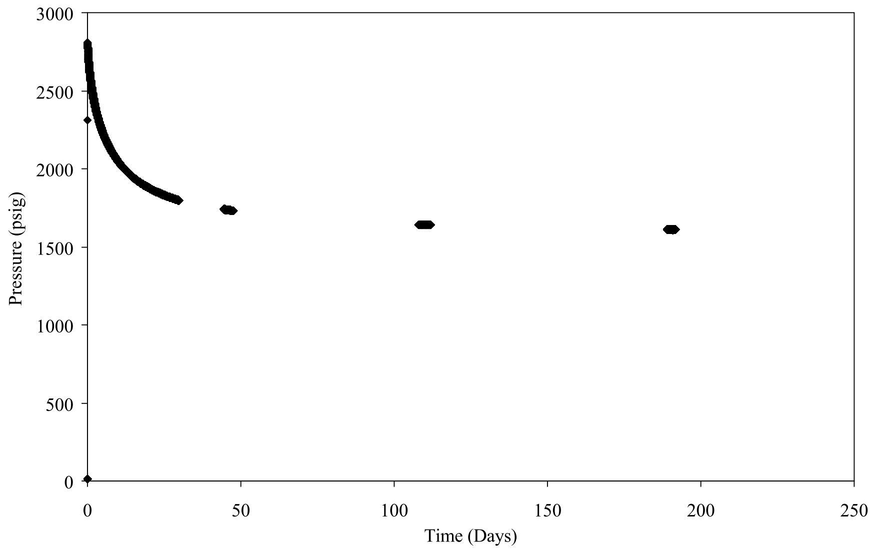

facility to monitor the amounts of fluids produced, as well as to collect periodic samples for chemical analyses. In addition, gas samples from well Stivason Federal 5 were also collected for chemical analyses. During the initial venting period, well Stivason Federal 4 produced fluids (gas and liquids) without any pumping. This period lasted for 9 days. After 9 days, the well stopped flowing, at which point a pumping unit had to be installed to produce the well further. The well has been on continuous production since that time and is currently on production. Figure 20 shows the amount of gas produced from the well for the first 3 months of venting and production. The daily rates of production of oil and water for the first 3 months of production are plotted in Figure 21. The gas production rates were significantly lower than the CO_2-injection rates. During the first 3 months of venting, only 17% of the total injected CO_2 was produced. The amounts of oil and water produced during venting and subsequent production phase were similar to production from the well during the pre-experiment days when it was actively produced. Figure 22 is a plot of the overall gas compositions of the samples collected from well Stivason Federal 4 during the venting and subsequent production operations. Figure 23 shows the trend in % CO_2 in the gas produced from Stivason Federal 4 until December 2004. Similarly, Figure 24 shows a plot of the gas composition of the samples collected from well

Figure 20. CO_2 production from well Stivason Federal 4 during the postsoak venting operation. Open-flow rates diminished rapidly during the first 200 h or 9 days of venting, after which, it would not flow. A pump was subsequently installed on the well, and production reached near equilibrium about 1 month after venting first began.

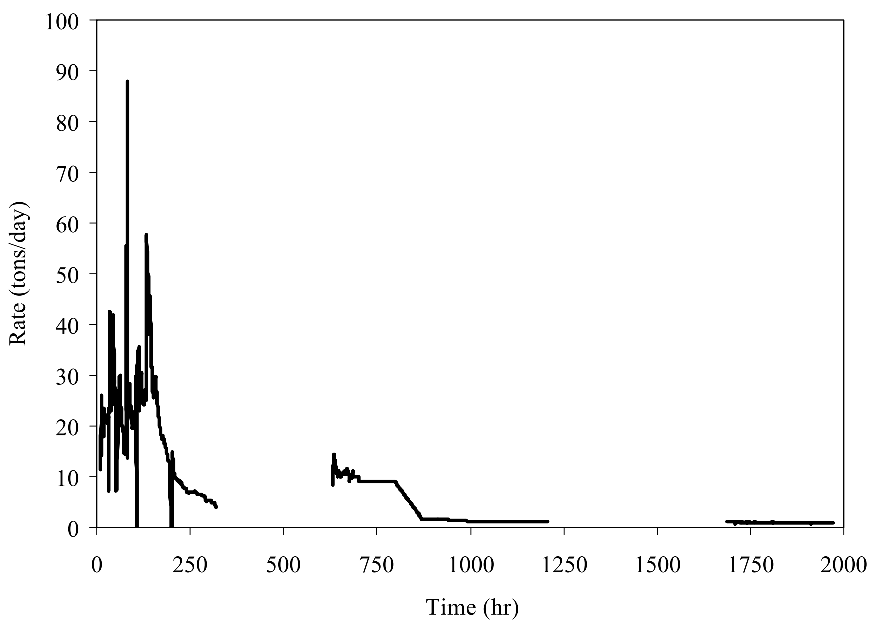

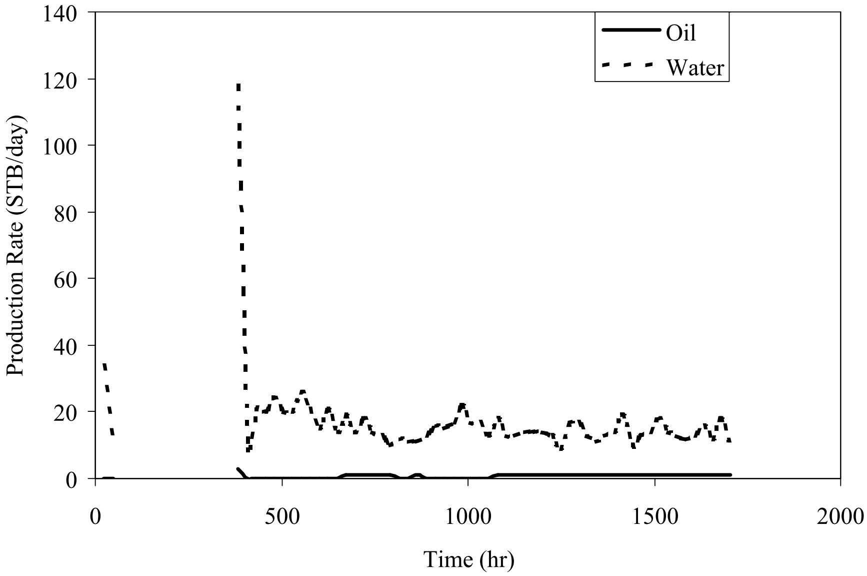

Figure 21. Water and oil production from well Stivason Federal 4 during the postsoak venting operation. The jump in water production subsequent to the installation of pump is caused by the accumulation of water during the shut-in period, during which the pump was installed.

Stivason Federal 5. The pre-CO_2-injection gas from the reservoir had less than 1% CO_2, whereas the gas samples collected from well Stivason Federal 4 during the venting operation was in the range of 95–99 mol% CO_2 through June 2004. The last two samples taken in October and December 2004 had 87.9 and 89.9 mol% CO_2, respectively. Samples from well Stivason Federal 5 do not show any presence of CO_2, which indicates that CO_2 had not migrated to well Stivason Federal 5 until December 2004. The oil and water production data from well Stivason Federal 5 and Sun Pearl 2, which are the only two actively producing wells from the West Pearl Queen reservoir interval, indicate that production from these wells has not been affected after the CO_2-injection experiment.

Geophysical Monitoring

As mentioned earlier, we used a time-dependent, three-dimensional seismic survey to monitor the CO_2 plume in the reservoir. So far, only the P-wave data have been processed, whereas interpretation of the S-wave data is still in progress. The P-wave seismic difference volume shows time-lapse amplitude anomalies in the reservoir interval east and southeast of the injection well. Figure 25 is a map of the RMS amplitude difference between the baseline and matched monitor survey over the West Pearl Queen reservoir interval. The contours that are overlain are the West Pearl Queen reservoir depth structure with a contour interval of 4 ft (1.22 m). The interpreted CO_2 distribution is highlighted and

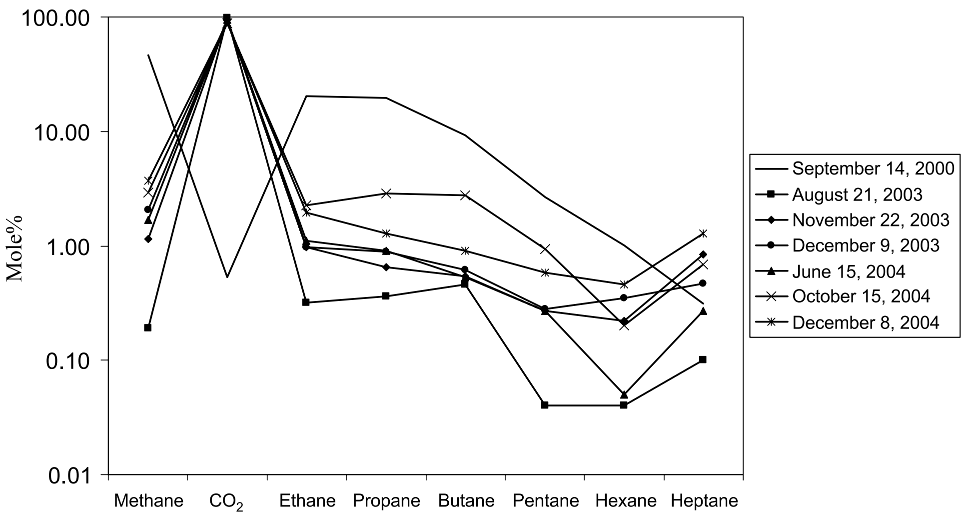

Figure 22. Composition of gas produced from well Stivason Federal 4 during CO_2 venting operation, showing the dramatic increase in CO_2 over the original gas compositions prior to injection.

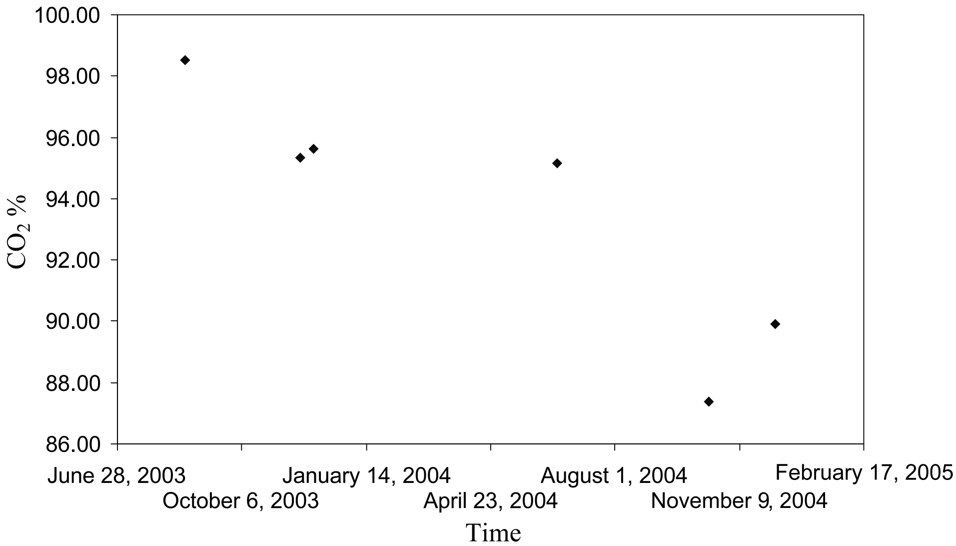

Figure 23. CO_2% in the gas produced from well Stivason Federal 4 decreased with time during CO_2 venting operation.

contained in the thicker, higher quality sands near the crest of the subtle anticline. The extent of the CO_2 plume as shown in the figure is consistent with observed CO_2 migration, based on production response from the wells in the vicinity, as well as the gas composition analyses from well Stivason Federal 5. The plume is also consistent with the reservoir structure and sand continuity between wells Stivason Federal 4 and Stivason Federal 5. Analysis of seismic data also shows that CO_2 has not migrated to formations other than the West Pearl Queen reservoir.

SUMMARY AND CONCLUSIONS

The observations and experimental results show that extensive reservoir characterization is necessary to understand and predict the impact of CO_2 injection on storage reservoirs. The response of the West Pearl Queen reservoir during the field experiment was significantly different than expected based on the preinjection characterization.

First, the observed CO_2-injection rate was much lower than the estimates based on earlier characterization work. This indicates that the permeability of the reservoir to CO_2 injection is significantly different than the laboratory values measured on core samples prior to this project. The static and dynamic laboratory experiments showed that geochemical interaction between CO_2 and West Pearl Queen sandstone could result in the migration of fines and decreased permeability, although more research is necessary to confirm that permeability changes observed in cores and in the field are the result of the same process. Second, the log analyses indicated that West Pearl Queen reservoir is continuous between the injection well (Stivason Federal 4) and the monitoring well (Stivason Federal 5). Numerical simulations with models based on the log analyses

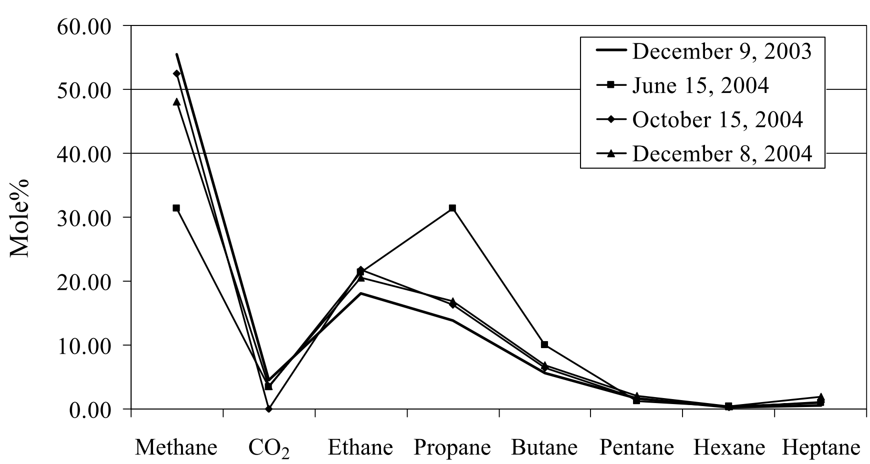

Figure 24. Composition of gas produced from well Stivason Federal 5. Mole % of CO_2 in the produced gas from this well indicates that injected CO_2 has not migrated to the well until at least December 8, 2004, approximately 2 yr after CO_2 injection began in well Stivason Federal 4.

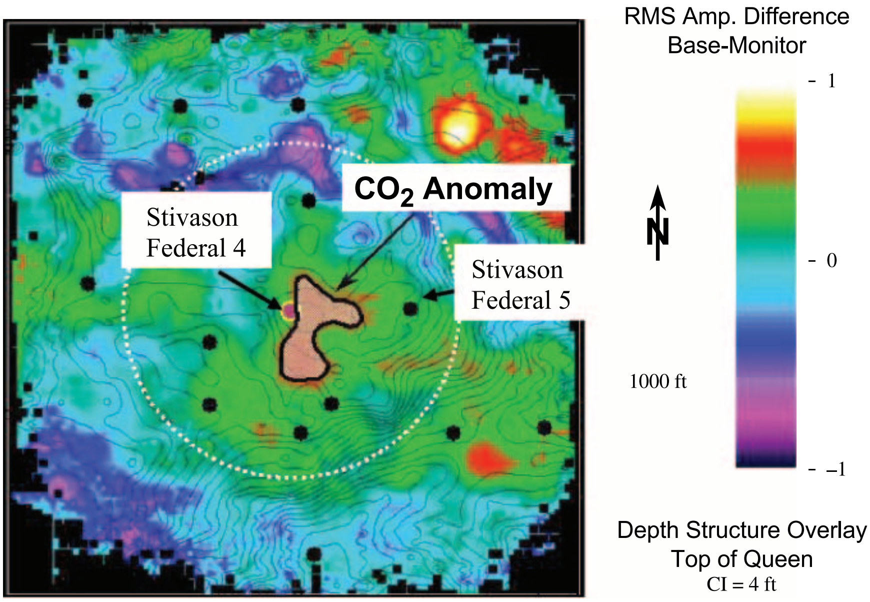

Figure 25. A map of RMS (root-mean-squared) amplitude difference between baseline and monitor three-dimensional, multidimensional surveys. The difference between the pre- and postinjection maps is taken as an indication of the probable location of the injected CO_2.

indicated that response of CO_2 injection in well Stivason Federal 4 would be observed in well Stivason Federal 5 in about 6 months. However, the observed production response during the field experiment as well as the geologic interpretation based on the seismic data imply that the reservoir is not continuous between the two wells. Comparison of the structure contours in Figure 2 (which were generated from well-log picks) and the structure interpreted from geophysical data (Figure 7) suggests that the reservoir geologic heterogeneity is not completely captured with analyses based on the log data alone. This project clearly demonstrates the importance of capturing the interwell heterogeneity for monitoring purposes. Third, the rate of production and the cumulative production during the initial 3 months of venting were significantly lower than expected. This indicates possible formation damage near the wellbore. It is also possible that the injected CO_2 dissipated away from the wellbore during the soak period into porosity not connected to the monitoring and production well.

Geophysical monitoring using P-wave analysis of the three-dimensional multicomponent seismic data shows an anomaly that may indicate the presence of CO_2. We are currently analyzing S-wave data to support this conclusion. This study shows the applicability of the surface seismic method for detecting a CO_2 plume, although the amount of CO_2 injected was small and individual zones were thin.

The laboratory experiments also provided some valuable results. Although dawsonite is a potential geochemical reaction product in sandstone reservoirs, this mineral was not formed during the laboratory experiments. Understanding the kinetics of dawsonite formation is critical for sequestration in sandstone reservoirs for two reasons. First, dawsonite is an important sink for CO_2, and second, its formation can also lead to irreversible and potentially damaging changes in reservoir properties such as permeability and porosity.

The results described in this study provide a basis that can be used to perform further studies to evaluate depleted oil reservoirs as a sequestration option. Our conclusions, combined with those of additional observations in this and other similar studies, should allow predictions on the long-term fate of CO_2 in depleted sandstone oil reservoirs.

REFERENCES CITED

Fetter, C. W., 1999, Contaminant hydrogeology: Upper Saddle River, New Jersey, Prentice-Hall, 171 p.

Holley, C., and J. Mazzullo, 1988, The lithology, depositional environments, and reservoir properties of sandstones in the Queen Formation, Magutex North, McFarland North, and McFarland fields, Andrews County, Texas, *in* B. K. Cunningham, ed., Permian and Pennsylvanian stratigraphy, Midland Basin, west Texas: Studies to aid hydrocarbon exploration: Permian Basin Section-SEPM Research Seminar No. 1, Publication 88-28, p. 55–63.

Knauss, K. G., and T. J. Wolrey, 1986, Dependence of albite dissolution kinetics on pH and time at 25°C and 70°C: Geochimica et Cosmochimica Acta, v. 50, no. 11, p. 2481–2497.

Lichtner, P. C., 2001, FLOTRAN user manual. LA-UR-01-2349: Los Alamos, New Mexico, Los Alamos National Laboratory, 172 p.

Malicse, A., and J. Mazzullo, 1990, Reservoir properties of the desert

Shattuck Member, Caprock field, New Mexico, *in* J. H. Barwis, J. G. McPherson, and J. R. J. Studlick, eds., Sandstone petroleum reservoirs: Casebooks in earth science: New York, Springer-Verlag, p. 133–152.

Mazzullo, J., A. Malicse, and J. Siegel, 1991, Facies and depositional environments of the Shattuck Sandstone on the northwest shelf of the Permian Basin: Journal of Sedimentary Petrology, v. 61, p. 940–958.

Mungan, N., 1992, Carbon dioxide flooding as an enhanced oil recovery process: Journal of Canadian Petroleum Technology, v. 31, p. 13–15.

Rimstidt, J. D., and H. L. Barnes, 1980, The kinetics of silica-water reactions: Geochimica et Cosmochimica Acta, v. 44, no. 11, p. 1683–1699.

Xu, T., J. A. Apps, and K. Pruess, 2003, Reactive geochemical transport simulation to study mineral trapping for CO_2 disposal in deep arenaceous formations: Journal of Geophysical Research, v. 108, no. B2, p. 2071.